Stimulated Compton Scattering from Preformed Underdense Plasmas

W. P. Leemans, C. E. Clayton, K. A. Marsh, and C. Joshi
Electrical Engineering Department, University of California, Los Angeles, California 90024
(Received 29 January 1991)

The electron-density-fluctuation spectra induced by stimulated Compton scattering (SCS) are directly observed for the first time. A CO_2 laser is focused into plasmas with densities n_e spanning $(0.4-6)\times10^{16}$ cm^{-3}. The fluctuations corresponding to backscatter are probed using Thomson scattering. At low n_e, the scattered spectrum peaks at a frequency shift $\Delta\omega=kv_e$ and appears to be in a linear convectively saturated regime. At the highest n_e, a nonlinear saturation of the SCS instability is observed possibly due to a self-induced perturbation of the electron distribution function.

PACS numbers: 52.35.Mw, 52.40.Nk

The induced scattering of electromagnetic waves by resonant electrons in a plasma, known as stimulated Compton scattering [1-3] (SCS), is a problem of fundamental importance in plasma physics and has applications in laser fusion, laser-driven accelerators [4], free-electron lasers, and tunnel ionization of gases. Historically, SCS has been of interest as a plasma-heating mechanism for low-density plasmas where other mechanisms such as inverse bremsstrahlung may be ineffective. The spectrum of SCS-induced fluctuations can provide both density and temperature information about the plasma. In this Letter, the electron-density-fluctuation spectra induced by SCS are directly observed for the first time. We show that at low densities this kinetic instability stays in the linear convective regime. However, as the density is increased a nonlinear saturation is seen to occur.

The SCS instability (off electrons) is the low-density or high-temperature—or large $k\lambda_{De}$—limit of stimulated Raman scattering [1] (SRS). Here k is the wave number of the density fluctuation responsible for the scattered light, $\lambda_{De}=(k_BT_e/4\pi n_e e^2)^{1/2}$ is the plasma Debye length, k_BT_e is the electron temperature, and n_e is the electron density. In the SRS instability, the pump electromagnetic wave, with wave vector $\mathbf{k}_0$ and frequency ω_0, scatters off an instability-generated electron plasma wave. In the SCS case, the electron plasma wave is heavily Landau damped and the pump and scattered light waves interact directly with the resonant thermal plasma electrons rather than through a collective mode of the plasma. Another consequence of the plasma mode being heavily damped is the experimental inaccessibility of this instability. One needs a very strong pump and sensitive diagnostics to observe significant levels of SCS density fluctuations. This alone explains the lack of experimental data on the SCS instability. The only previous experimental observation was by Drake *et al.* [5]. In their experiment exploding-foil plasmas were used. The Compton instability was studied by monitoring a *single* wavelength of the scattered light close enough to the pump-laser wavelength to ensure that the radiation was emitted by a low-density plasma (high $k\lambda_{De}$). This is in contrast to the experiment reported here where it is precisely the details of the scattered *spectrum* that allow us to draw conclusions regarding the physics of the interaction. In this experiment an intense CO_2 laser drives SCS in a low-density, preformed plasma. The density fluctuations are probed using Thomson scattering of a visible probe laser beam.

In a finite-length plasma, Compton scattering can be described as the convective amplification, by the Compton instability, of some noise-level spectrum. The noise spectrum is taken to be thermal Thomson scattering [6] off the preformed plasma. The spatial growth rate $\kappa(\Delta\omega,k\lambda_{De})$ for backscattering modes with $\mathbf{k}\approx2\mathbf{k}_0$ is given by [1]

$$\kappa(\Delta\omega,k\lambda_{De})=2\left(\frac{v_0}{c}\right)^2\frac{\omega_0}{c}\mathrm{Im}\frac{\chi_e(\Delta\omega,k\lambda_{De})}{1+\chi_e(\Delta\omega,k\lambda_{De})}, \quad (1)$$

where v_0/c is the normalized electron quiver velocity in the electric field of the pump and $\chi_e(\Delta\omega,k\lambda_{De})$ is the usual electron susceptibility. Equation (1) is valid away from the strongly driven regime which for our densities and laser intensities is satisfied [1]. Also, since the SCS fluctuations propagate in a direction normal to the incident laser electric field, i.e., $\mathbf{k}\cdot\mathbf{v}_0=0$, the expression for $\chi_e(\Delta\omega,k\lambda_{De})$ is thought not to be affected for the case where $v_0>v_e$, where $v_e=(k_BT_e/m)^{1/2}$ is the electron thermal velocity [7]. However, this issue clearly needs further theoretical attention. The scattered CO_2 power $P_s(\Delta\omega,L)$ is just $P_s(\Delta\omega,L)=P_N\exp(\kappa L)$, where P_N is the noise spectrum, taken to be due to thermal Thomson scattering off the preformed plasma [6] and L is the length of the convective amplifier. Since the Thomson-scattering probe measures the density fluctuations associated with the CO_2-laser backscatter at one point in space z', the spectrum is then of the form

$$P_{TS}(\Delta\omega,t)=\begin{cases}AP_N(\Delta\omega,k\lambda_{De},t=0)\exp[\kappa(\Delta\omega,k\lambda_{De})ct] & \text{for } t<T, \quad (2a)\\ AP_N(\Delta\omega,k\lambda_{De},t=0)\exp[\kappa(\Delta\omega,k\lambda_{De})cT] & \text{for } t>T, \quad (2b)\end{cases}$$

where we have assumed the group velocity of the light wave to be c for the underdense plasmas, T is the transit time of the scattered wave to the point z', and A is a fitting parameter. The effect of increasing $k\lambda_{De}$ beyond about 0.3 in Eqs. (2a) and (2b) is to significantly broaden the range of frequency shifts $\Delta\omega$ which have significant growth, leading to scattered spectra with widths becoming on the order of the maximum shift.

The experimental apparatus is as follows. The laser driving the instability is a CO_2 laser operating at 10.6 μm with a measured output-pulse rise time of about 100 ps and a full width at half maximum of about 270 ps. For these experiments the peak power is varied up to about 150 GW, giving a focused intensity of about 10^{14} W/cm^2 in a measured spot size of 340 μm diameter. The plasma source is a 1-cm-long, multiple-cathode, pulsed (10 μs), high-current (2.5 kA) arc discharge [8] in hydrogen (Figs. 1 and 3) or argon (Fig. 2) gas. The resulting electron density can be varied from less than 10^{15} to more than 10^{17} cm^{-3} by varying the fill pressure of the gas, the peak discharge current, and the elapsed time between the start of the discharge and the CO_2 laser pulse. For elapsed times larger than 10 μs, the arc plasma is fully ionized to $Z=1$. In the Thomson-scattering setup, the frequency-doubled Nd-doped yttrium aluminum garnet laser probe beam (150 mJ, 5 ns) and the scattered-light collection optics are arranged to phase match to density fluctuations with wave number $(2\pm0.2)\mathbf{k}_0$. The scattered light is sent through a spectrograph, with a spectral dispersion of 8 Å/mm, to the 10-mm-long slit of a streak camera. The temporal (spectral) resolution of the system is 10 ps (0.2 Å). For time-integrated measurements, a linear detector array replaces the streak camera. A spectrometer and pyroelectric linear array are used to record the spectrum of the CO_2 backscatter signal.

To access a parameter space which is unambiguously in the Compton regime, we reduced the arc-plasma density until the scattered signals appeared broad on the linear array detectors indicating, as described by Eq. (2), that $k\lambda_{De}$ is larger than 0.3. In Figs. 1(a) and 1(b), time-integrated CO_2 backscatter and Thomson-scatter spectra, respectively, are shown from low plasma densities. Both spectra exhibit a sharp edge on the high-frequency side and a gradual reduction on the low-frequency side as expected from the frequency dependence of the growth rate. This is in contrast to the scattered signals from high-density plasmas with $k\lambda_{De}<0.3$ which show a sharp, instrument-limited peak characteristic of the Bohm-Gross frequency shift [Fig. 1(c)]. To quantitatively compare the experiment with the linear theory, we time resolved the Thomson-scattering data. Figure 2(a) shows the frequency spectrum of the Thomson-scattered light versus time. We see a feature with an approximately 8-Å redshift (28 cm^{-1}) from the 5320-Å probe light which we identify as light scattered by electron density fluctuations associated with SCS. This feature is followed in time by

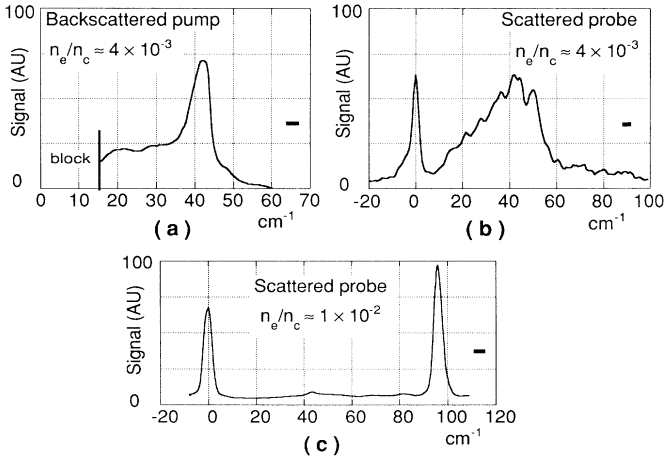

FIG. 1. Time-integrated (a) CO_2 backscatter spectrum and (b) probe-beam Thomson-scatter spectrum from a low-density hydrogen plasma, and (c) time-integrated probe-beam Thomson-scatter spectrum from a high-density plasma. The three spectra are from different laser shots. The peaks at zero shift are from SBS [physically blocked in (a)]. The horizontal bars indicate the instrument width.

an essentially unshifted feature due to ion acoustic waves driven by stimulated Brillouin scattering [9] (SBS). Note that the lack of a blueshifted feature verifies that these are laser-driven density fluctuations (nonthermal) propagating in the same direction as the CO_2 laser beam.

To fit the data by a linear SCS theory, lineouts were taken at a time before convective saturation, as shown in Fig. 2. Equation (2a) is used to fit the data. An enhanced noise level about 5 times the nominal thermal level was used as it produced a better fit to the data. Values for $k\lambda_{De}$ and n_e are adjusted to fit the shape and scale of the theoretical spectrum to the experimental spectrum. Using Eq. (2a) with $T=25$ ps (the transit time for the scattered light wave), v_0/c is adjusted to scale the peak amplitude of the theoretical spectrum to that of the measured spectrum. Effectively, v_0/c is some average value over the growth time. The parameters which best fit the data are $v_0/c\approx0.08$, $n_e\approx4\times10^{15}$ cm^{-3}, and $k\lambda_{De}\approx1.5$ so that $T_e\approx120$ eV. The inferred plasma density agrees roughly with line-average interferometric density measurements made under similar arc-discharge conditions. We do not expect the density to change due to collisional or tunneling ionization since the rates for these processes are too slow. Since $k\lambda_{De}$ is about 1.5, the phase velocity v_ϕ for the strongest mode is $v_\phi\approx1.0v_e$ putting it right in the bulk of the electron distribution function. The ponderomotive potential from the beating of the pump and scattered electromagnetic waves is thus at a velocity where it can directly manipulate the electron distribution function. However, for this very low-density case, the SCS reflectivity is too low to allow, through the Manley-Rowe condition, much transfer of

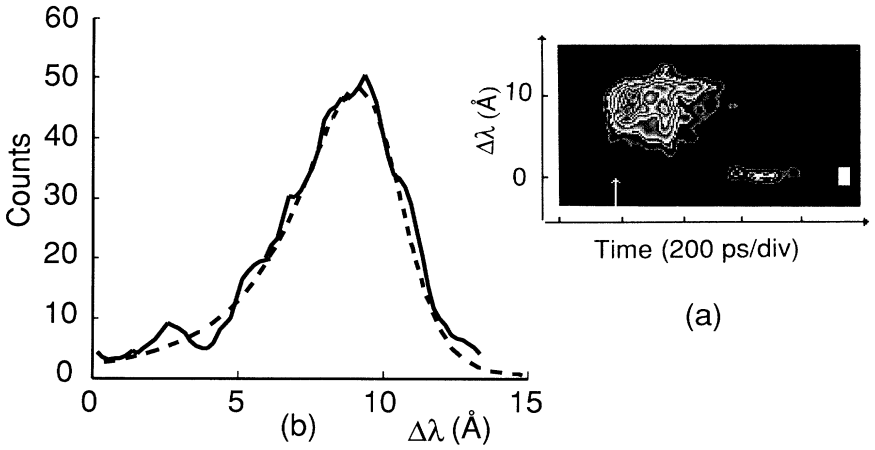

FIG. 2. (a) Streak-camera image of the Thomson-scattered probe beam in an argon plasma. Although not shown here, there was no blueshifted spectral feature visible in the original data. The white bar indicates the location of a 100× attenuator for SBS. The peak intensity is 1.5×10^{14} W/cm^2. (b) Lineout of streak data (solid curve) taken along the direction of the arrow and best fit from Compton theory (dashed curve).

power to the plasma. The scattered spectrum does not show a pronounced variation with time indicating that the electron distribution function is not being significantly altered.

The situation is quite different at higher densities and higher reflectivities. Figure 3(a) shows a streak-camera image of the $2k_0$ density-fluctuation spectrum for a 10-times-higher plasma density and a 3-times-higher laser intensity than in Fig. 2(a). We see the instability start off at a 23-Å redshift (78 cm^{-1}). From a lineout through the spectrum, taken at a time when the signal has reached about 60% of the peak level (25 ps into the scattered pulse), we infer the parameters $v_0/c\approx0.02$, $n_e\approx6\times10^{16}$ cm^{-3}, and $k\lambda_{De}\approx0.6$, so that $T_e\approx200$ eV and $v_\phi/v_e\approx2.2$. Examination of the inner or more intense contours of Fig. 3(a) shows that the spectrum makes a fairly sudden turn towards lower frequency and the lower frequencies become suddenly enhanced at about the same time that the original 23-Å feature saturates. Lineouts of Fig. 3(a) representing the time histories of four frequencies (as marked by arrows on the streak image) are shown in Fig. 3(b). We see the enhancement of the growth rate of the 22-Å-shifted light coincident with the saturation of the 23-Å feature. Also, we see the

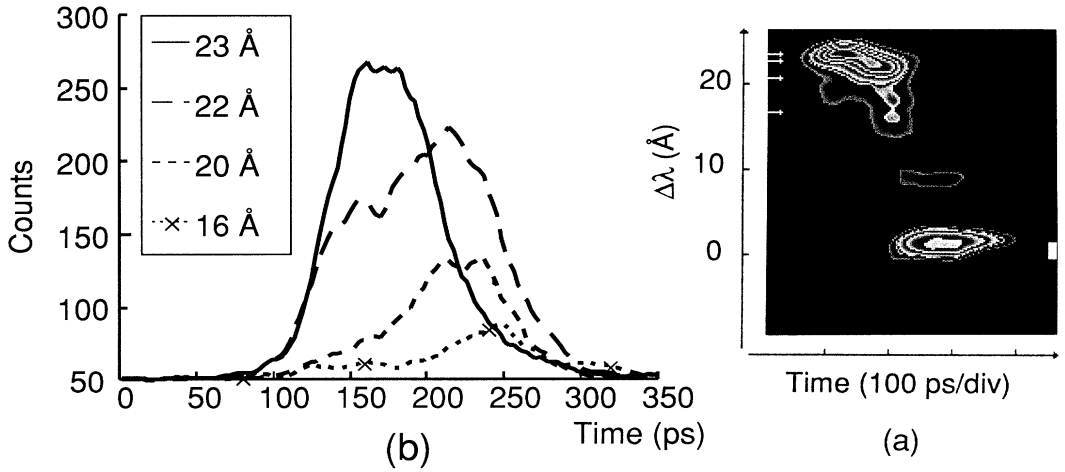

FIG. 3. (a) Streak-camera image of the Thomson-scattered probe beam in a hydrogen plasma. Although not shown here, there was no blueshifted spectral feature near 20 Å visible in the original data. (The feature at 8 Å of redshift, which does have a blueshifted counterpart, is due to mode coupling of driven fluctuations with the SBS acoustic wave [10] due to the presence of a weak second frequency in the laser pulse for this particular data shot.) The white bar indicates the location of a 100× attenuator. The peak intensity is 5×10^{14} W/cm^2. (b) Lineouts taken along the direction of the four arrows in (a).

smaller frequency shifts peaking progressively later in time. The 16-Å-shifted light peaks well after the 23-Å feature saturates indicating that the saturation of the 23-Å feature was not due to an absence of the pump. The frequency spectrum during the final state of the instability is similar to the large-$k\lambda_{De}$ spectrum of Fig. 2(a) in that it extends down to $\Delta\omega = kv_\phi \approx 1.1kv_e$. That is, the instability involves particles in the bulk of the distribution function. It should be noted that while Compton scattering is occurring in the experiment the ratio v_0/v_e is typically 3 and therefore filamentation may also be operative. Any density reduction due to self-focusing will shift the Thomson spectrum from Compton-induced density fluctuations towards lower frequencies (Fig. 3). However, the simultaneous broadening of the spectrum as the higher frequencies saturate cannot be accounted for by invoking self-focusing and one is led to look for another saturation mechanism.

Equation (1) suggests that one way to saturate the instability is to change the electron distribution function $f(v)$ and therefore the electron susceptibility χ_e such that the growth rate $\gamma(\Delta\omega, f(v))$ no longer has a resonance at the original 23-Å shift but perhaps at a lower frequency shift. This could account for both the saturation of the scattered light signal at the original frequency shift and the appearance of a signal at new frequency shifts at later times, as seen in Fig. 3. To test this idea we ran the electromagnetic particle-in-cell computer code WAVE to simulate the experiment. A one-spatial-dimensional simulation with $k\lambda_{De} = 0.6$ was run. The backscattered frequency spectrum was monitored as was the longitudinal electron distribution function. In this simulation, the peak backscatter signal built up and saturated while, at the same time, the longitudinal distribution function became asymmetric, with a tail being pulled out on the side moving along $\mathbf{k}_0$. This is due to momentum deposition to electrons with a velocity near $\mathbf{v}_\phi$ from the reflecting pump photons. The detailed time evolution of the scattered light spectra looked very similar to the experimental data of Fig. 3(a). The signal started out narrow band at a frequency corresponding to that of the maximum growth rate for the unperturbed, Maxwellian plasma. As this frequency component saturated, the peak moved to lower frequency shifts (shifting by a factor of about 0.85) and the bandwidth became broader ($\Delta\omega/\omega \approx 30\%$). The power at the original frequency fell after saturation, as it did in the experiment. This could be due to phase mixing of the bunched electrons contributing to that particular mode, once that mode is no longer driven. The reason that the mode is no longer driven can be seen from the theoretical growth rate of Eq. (1). When the electron distribution function is perturbed, the poles of the function move to new frequencies. In fact, when we numerically solve for χ_e using the final electron distribution function from WAVE as an input and use the result in Eq. (1), we find that the growth-rate peak has indeed shifted towards lower frequency and has become broader. Thus, it seems that Compton scattering is self-limiting in low-density plasmas because the momentum absorbed in the instability is typically enough to perturb the distribution function and thereby turn the instability off at any particular frequency [3]. Although SRS could grow in the flattened region of $f(v)$, phase-space turbulence associated with particle trapping can account for the absence of SRS in both experiment and simulation. The SCS-induced CO_2 reflectivity was 10^{-4}.

We should note that, with the very short 100-ps rise time for the laser pulse, the electron-time-scale processes occur before SBS has a chance to grow, thus experimentally decoupling the two instabilities. Typically, SBS comes up late in the SCS pulse or even well after the SCS has shut off. Thus SCS is not terminated by SBS.

In conclusion, we have reported the first detailed spectral measurements of stimulated Compton scattering from a preformed plasma. For low density, the observed density-fluctuation spectra seem to be convectively saturated and have the predicted large spectral bandwidth throughout the time of interaction. The scattered light peaks at a frequency shift $\Delta\omega$ corresponding to a phase velocity about equal to the electron thermal velocity. For higher density, an initially narrow spectrum is seen to saturate and evolve into broadband Compton scattering with frequency shifts once again near kv_e. Using the code WAVE as a guide, we suggest that the saturation is due to a reflectivity-induced modification of the electron distribution function.

We would like to acknowledge useful discussions with Dr. W. B. Mori, Dr. T. Katsouleas, Dr. R. P. Drake, Dr. K. G. Estabrook, and Dr. B. F. Lasinski. This work was supported by the U.S. Department of Energy under Contract No. DE-AS03-83-ER40120 and the LLNL University Research Program.

[1] J. F. Drake *et al.*, Phys. Fluids **17**, 778 (1974).
[2] A. G. Litvak and V. Yu. Trakhtengerts, Zh. Eksp. Teor. Fiz. **60**, 1702 (1971) [Sov. Phys. JETP **33**, 921 (1971)]; A. T. Lin and J. M. Dawson, Phys. Fluids **18**, 201 (1975).
[3] J. R. Albritton, Phys. Fluids **18**, 51 (1975).
[4] C. Joshi *et al.*, Nature (London) **311**, 525 (1984).
[5] R. P. Drake *et al.*, Phys. Rev. Lett. **64**, 423 (1990).
[6] J. Sheffield, *Plasma Scattering of Electromagnetic Radiation* (Academic, New York, 1975).
[7] J. Bernard *et al.*, Phys. Rev. A **39**, 2549 (1989).
[8] C. E. Clayton (to be published).
[9] D. W. Forslund *et al.*, Phys. Fluids **18**, 1002 (1975).
[10] C. Darrow *et al.*, Phys. Rev. Lett. **56**, 2629 (1986).

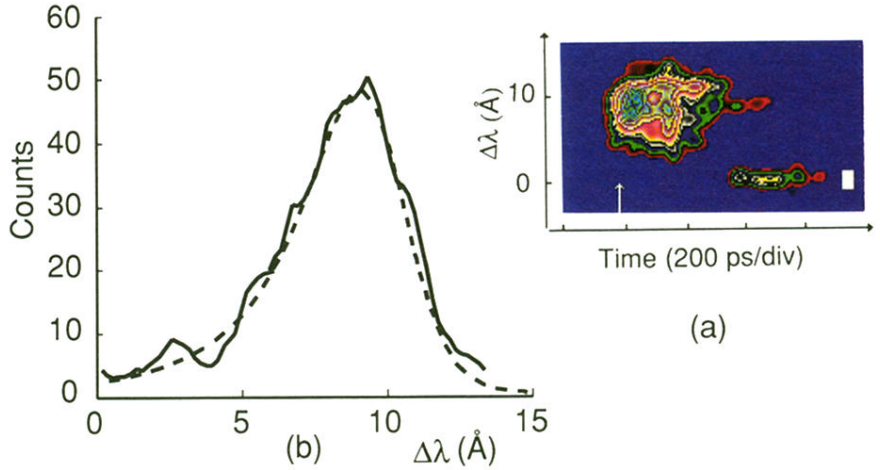

FIG. 2. (a) Streak-camera image of the Thomson-scattered probe beam in an argon plasma. Although not shown here, there was no blueshifted spectral feature visible in the original data. The white bar indicates the location of a 100× attenuator for SBS. The peak intensity is 1.5×10^{14} W/cm^2. (b) Lineout of streak data (solid curve) taken along the direction of the arrow and best fit from Compton theory (dashed curve).

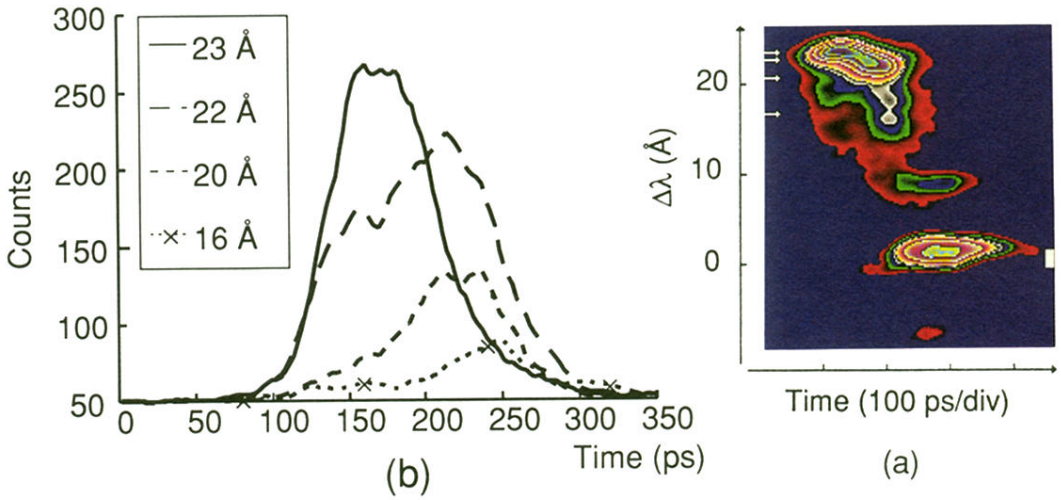

FIG. 3. (a) Streak-camera image of the Thomson-scattered probe beam in a hydrogen plasma. Although not shown here, there was no blueshifted spectral feature near 20 Å visible in the original data. (The feature at 8 Å of redshift, which does have a blueshifted counterpart, is due to mode coupling of driven fluctuations with the SBS acoustic wave [10] due to the presence of a weak second frequency in the laser pulse for this particular data shot.) The white bar indicates the location of a 100× attenuator. The peak intensity is 5×10^{14} W/cm^2. (b) Lineouts taken along the direction of the four arrows in (a).